INSTITUTE OF PHYSICS PUBLISHING JOURNAL OF PHYSICS B: ATOMIC, MOLECULAR AND OPTICAL PHYSICS

J. Phys. B: At. Mol. Opt. Phys. **36** (2003) 2371–2383 PII: S0953-4075(03)59214-8

Electron-impact excitation of the $(n-1)d^9ns^2np$ autoionizing states of cadmium ($n = 5$) and zinc ($n = 4$)

B Predojević[1,2], D Šević[1], V Pejčev[1,3], B P Marinković[1] and D M Filipović[1,4]

[1] Institute of Physics, PO Box 57, 11001, Belgrade, Serbia and Montenegro
[2] Faculty of Natural Sciences, University of Banja Luka, Republic of Srpska, Bosnia and Herzegovina
[3] Faculty of Natural Sciences, University of Kragujevac, Serbia and Montenegro
[4] Faculty of Physics, University of Belgrade, PO Box 368, 11001, Belgrade, Serbia and Montenegro

Received 31 January 2003
Published 23 May 2003
Online at stacks.iop.org/JPhysB/36/2371

Abstract

Electron-impact excitation of the $5\,^3P_1$ (12.062 eV) and $5\,^1P_1$ (12.810 eV) $4d^95s^25p$ autoionizing states of Cd has been experimentally investigated at incident electron energies (E_0) from 15 to 60 eV and scattering angles (θ) up to 40° (at $E_0 = 40$ eV, $\theta = 2°$–150°). The absolute differential cross sections (DCSs) at $E_0 = 40$ eV were determined through normalization to the optical oscillator strengths. These DCSs were extrapolated to 0° and 180° and numerically integrated to yield integral, momentum transfer and viscosity cross sections. Energy-loss spectra for Cd were recorded from 11 to 18 eV, and 22 autoionizing states were identified at different impact energies. Electron-impact excitation of the $3d^94s^24p$ autoionizing states was observed in energy-loss spectra of Zn at $E_0 = 20, 60, 80$ and 100 eV (θ up to 10°). The DCSs for Cd could not be compared with other results, because there are no available data in literature. The autoionizing energy levels and line widths are in good agreement with existing experimental and calculated values.

1. Introduction

Knowledge of line intensities in autoionizaton spectra for both 'optically allowed' and 'optically forbidden' transitions is used to determine physical parameters of astrophysical plasmas (Doschek 1985). At present, detailed knowledge of the Cd and Zn structure is of particular interest because of their use in metal-vapour lasers (Ivanov *et al* 1990).

Autoionizing spectra of Cd ($n = 5$) and Zn ($n = 4$) are dominated by single inner-electron transitions $(n-1)d^{10}ns^2 \rightarrow (n-1)d^9ns^2mp$, where $m \geqslant n$. The transitions mentioned above

were observed initially in photoabsorption spectra carried out by Beutler (1933) and Beutler and Guggenheimer (1933) respectively. Berkowitz and Lifshitz (1968) measured peaks in the photoionization continuum of Cd, corresponding to $4d^9 5s^2 mp$, $m \geqslant 5$ states with $J = 1$. Garton and Connerade (1969) have extended the measurements and found new examples of 'resonance' lines in absorption spectra of the group IIb atoms. Marr and Austin (1969a, 1969b) measured VUV absorption cross sections and determined optical oscillator strengths (OOSs) for several series of transitions in Cd and Zn, respectively. Using an electron synchrotron as a background continuum source, Mansfield (1978) recorded the Cd single-inner-electron excitation spectrum together with the double-valence excitation spectrum and found that there are no perturbations due to coincidences in the energies of states. In the Zn spectra, Mansfield and Connerade (1978) found regularities similar to those in Cd, but they found much closer lines and also perturbation of high series members of the double-valence excitation spectrum by single inner-electron transitions to the $3d^9 4s^2 5p$ autoionizing states.

Studies of ejected-electron spectra resulting from electron excitation of Cd autoionizing levels were reported initially by Wickes *et al* (1971). They observed the spectra for $E_0 = 400$ eV perpendicularly to the incident electron beam. Newell *et al* (1973) observed the spectra at the same angle, but for E_0 between 15 and 40 eV. These spectra show a multiplet structure observed previously neither at higher energies nor in the ultraviolet photoabsorption. In ejected-electron spectra of Cd autoionizing states excited by $E_0 = 15$–400 eV electrons, Pejčev *et al* (1977a, 1977b) observed 64 lines at ejected-electron angles up to 110°. Back *et al* (1981) observed 83 lines in the spectra of Zn autoionizing states excited by $E_0 = 16$–300 eV electrons.

Scattered electron intensity observation is a powerful method to investigate excitation of atomic autoionizing states, in two ways: by direct angular distribution measurement and by recording the energy-loss spectra. Both of them have been used in this work. If a target atom is in the ground state, lines in electron energy-loss spectra are attributed to its excited states, without any confusion due to decay channels in autoionization. A difference between the ejected-electron and electron energy-loss spectra of Cd has been clearly demonstrated by Wickes *et al* (1971). Electron-impact excitations of the Zn autoionizing states are restricted to investigation by Trajmar and Williams (1976). We will discuss the results of these authors in detail in section 4.

The autoionizing $(n-1)d^9 ns^2 np$ energy levels have been calculated by Wilson (1968) using Hartree–Fock solutions for Cd, without taking configuration mixing effects into account; Martin *et al* (1972), using an intermediate-coupling scheme for Zn, Cd and Hg; Martin (1984), applying experimental OOSs in the single-configuration approximation for the same atoms; Mansfield (1981), through multiconfiguration Hartree–Fock (MCHF) interpretation of ejected-electron spectra for Zn, and Mansfield and Murnane (1985), in the MCHF analysis for Cd. Tabanli *et al* (2002) have studied Cd ($4d^9 5s^2 5p$, ^3P, ^1P and ^3D, $J = 1$) autoionizing states, motivated by the (e, 2e) experiment of Martin *et al* (1999), using the overlapping resonance treatment in their first-order distorted-wave calculation.

Kontros *et al* (2002) measured electron-impact ionization efficiency for Cd in the energy range $E_0 = 8$–16 eV. These authors do not explain a feature on the ionization efficiency curve at approximately 12.8 eV that could be attributed to the $^1P_1$ autoionizing state.

In section 2, we report the experimental procedure of differential cross section (DCS) measurements for electron-impact excitation of the $^3P_1$ and $^1P_1$ autoionizing states of Cd in a broad domain up to $\theta = 150°$. Details related to the metal-vapour sources, relevant for recording the energy-loss spectra of Cd and Zn, are also included. Results of the DCS and energy-loss measurements are shown in section 3. In section 4, details concerning both electronic structure and transitions observed in the Cd and Zn spectra are discussed, and a conclusion is given.

2. The experiment and procedure

The apparatus used for the measurements is a conventional cross-beam electron spectrometer described elsewhere (Filipović *et al* 1988). The optics of both the monochromator and analyser are very similar to that designed by Chutjian (1979). Doppler broadening of lines in electron energy-loss spectra is avoided because the electron beam is perpendicular to the atomic beam and because of the narrow beam geometry. All cylindrical electrostatic lenses are made of OFHC copper, which is gold plated, while hemispherical energy selectors and diaphragms are made of molybdenum. A channel electron multiplier is used for single-electron counting. The analyser can be positioned from $-30°$ up to $150°$ with respect to the mechanical zero. For each separate experiment, angular distribution of the scattered electron intensity, which is symmetric around the real zero, has been measured from $-20°$ to $+20°$. In this way, the zero scattering angle was determined with uncertainty of $0.5°$. Typical overall energy resolutions (as FWHM) were 50 meV for Cd, but approximately 140 meV for Zn to compromise with good signal intensity. The angular resolution of the spectrometer is estimated to be $1.5°$ in both cases. The energy scale was calibrated by measuring the position of the feature in the elastic scattering attributed to the threshold energy of the 5 ^{3}P excitation of Cd at 3.737 eV. A similar effect was seen in the elastic scattering by Zn if the resolution was as high as 40 meV. The structure at 4.03 eV, attributed to the 4 ^{3}P excitation threshold of Zn, was utilized for calibration of the energy scale in the case of Zn.

The metal-vapour source consists of a tubular stainless-steel crucible for Cd (Marinković *et al* 1991). In the case of Zn, the crucible was made of titanium, which is completely resistive to Zn vapour (Ross and Sonntag 1998). The crucible is placed in a stainless-steel cylinder co-axially wrapped with two resistive bifilar heaters (top and bottom) which enables the top of the system to be maintained at approximately 100 K higher than the bottom. This prevents clogging and minimizes dimer production. Monitoring of the temperature is carried out by two thermocouples, on the top and at the bottom of the crucible. To attain higher ultimate temperature and more stable operating conditions, a titanium foil around the cylinder and tantalum foil on its top end are mounted to reflect the thermal radiation back to the crucible. An additional outer cylinder is made of copper and its purpose is not only to be a radiation shield, but also to be a collimator for the metal vapour that turns into the solid state in a liquid-nitrogen cold trap mounted above the interaction region.

In the case of Cd, the experimental procedure was very similar to that reported earlier (Marinković *et al* 1991). Our measurements were performed at a temperature of 580 K for Cd of 99.95% purity. In the case of Zn, higher target density is desirable because of its lower excitation cross section values. Careful choice of the temperature is important because a feature due to double scattering of electrons after excitation of the same 4p (^{1}P$_1$) resonant state at 5.8 eV screens the autoionizing features in the vicinity of 11.6 eV. Zn (purity 99.9%) was firstly heated at about 800 K, but the temperature was decreased to 750 K at which the shape of the autoionizing spectrum was not temperature sensitive. Working temperatures for Cd and Zn mentioned above correspond to the metal-vapour pressures of 8 and 103 Pa respectively. The Cd beam effuses through a cylindrical channel in the cap with the aspect ratio $\gamma = 0.136$, and the Zn beam through the channel with $\gamma = 0.075$. The effective path-length correction factors (F) (Brinkman and Trajmar 1981) were calculated using the procedure described by Marinković *et al* (1991) for Cd. Absolute DCS values are determined through normalization of the relative values to the OOS, utilizing the forward scattering function (FSF) introduced by Avdonina *et al* (1997). Integral (Q_I), momentum transfer (Q_M) and viscosity (Q_V) cross sections are determined by numerical integration of DCSs after their polynomial extrapolation to $\theta = 0°$ and $180°$.

Lines in our Cd autoionizing energy-loss spectra were directly identified according to Mansfield and Murnane (1985). The spectrum between 11.7 and 13.2 eV was fitted using the χ^2 minimization procedure. We assumed that the isolated line at 12.062 eV is a convolution of our Gaussian apparatus function (FWHM equal to that of the elastic peak) and the symmetric component of a Shore (1967) line profile of the autoionizing state. For the unresolved feature near 12.81 eV, which contains $5\,^1P_1$ and $5\,^3D_1$ states, we performed decomposition into two log-normal profiles. More complete description of the line profiles involving interaction between individual resonances is generally possible using the overlap matrix parameter introduced by Mies (1968). But, it may be impossible to achieve it in a unique way, especially from limited experimental observations in electron spectroscopy with more complex transition rules than in optical spectroscopy. Instead of performing a sophisticated calculation, we decided simply to reproduce the obvious asymmetry of the spectral lines using the conventional log-normal function.

Lines in our autoionizing energy-loss spectra of Zn (between 11.0 and 12.5 eV) are identified according to Mansfield (1981). The lines are close one to another and detailed decomposition of the spectrum into the line components is more difficult than in the case of Cd.

3. Results

3.1. Differential and integrated cross sections

We have measured inelastic DCSs for electron-impact excitation of the $5\,^3P_1$ and $5\,^1P_1$ fine structure states of Cd with $4d^95s^25p$ electronic configuration, at $E_0 = 40$ eV and the angles θ from 2° to 150°. In a separate series of experiments, DCS measurements for both the $5\,^3P_1$ and $5\,^1P_1$ states were performed at $E_0 = 40$ eV and $\theta \leqslant 10°$ in steps of 2° (at $\theta = 0°$ DCSs are obtained by extrapolation). From these measurements the relative generalized oscillator strengths (GOSs) were obtained. Using the GOS (K^2) diagram (where K is the momentum transfer) FSFs for particular states were drawn and presented together with OOSs of 0.07 for the $5\,^3P_1$ state and 0.53 for the $5\,^1P_1$ state adopted from photoabsorption measurements by Marr and Austin (1969a) (figures 1(a), (b)). A normalized GOS has been achieved through displacement of our relative GOS at $\theta = 0°$ until its value attained that of the FSF at the corresponding K^2 value. The normalized-to-relative GOS quotient has then been used as the normalization factor for putting our relative DCS to the absolute scale.

The absolute DCSs for the $5\,^3P_1$ and $5\,^1P_1$ states are given in table 1. The errors arise from two sources: (a) uncertainties in our experimental values, and (b) uncertainty in the normalization procedure. Uncertainties in our experimental values reflect the uncertainty of relative DCS. This arises from a statistical error (shown in parentheses), uncertainty of θ (0.03), uncertainty of E_0 (0.01) and uncertainty of F (0.06). On the other hand, uncertainty in the normalization arises from uncertainty of the OOS obtained by Marr and Austin (1969a) directly from the cross sectional data. Because uncertainty on these absolute cross sections for all tabulated values (including those of much smaller intensities than for the $5\,^3P_1$ and $5\,^1P_1$ states) is less than 0.20, we estimated 0.20 as the uncertainty in our normalization procedure. The total absolute errors are given in separate columns in a form convenient for further use.

The integrated cross sections are obtained by polynomial extrapolation of the absolute DCSs to $\theta = 0°$ and 180°, and numerical integration, as follows.

The integral cross section is obtained using the equation

$$Q_I = 2\pi \int_0^{\pi} \mathrm{DCS}(\theta) \sin\theta \, \mathrm{d}\theta, \tag{1}$$

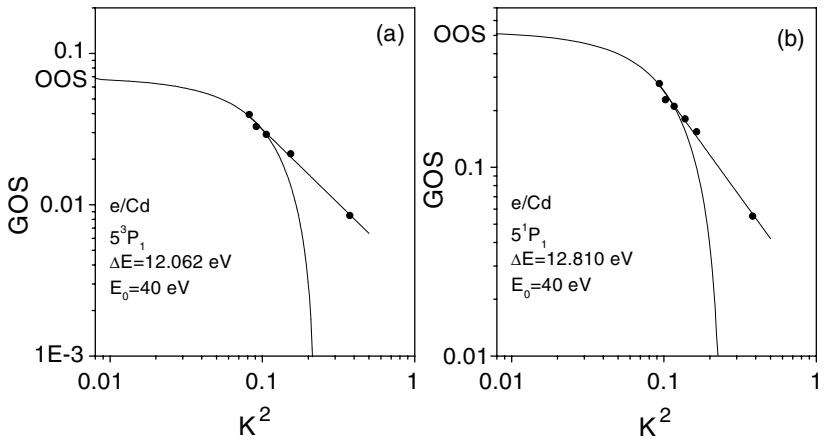

Figure 1. GOS for electron-impact excitation of the autoionizing states of Cd at 40 eV incident electron energy: (a) $4d^9 4s^2 5p\ ^3P_1$ (energy-loss $\Delta E = 12.062$ eV) and (b) $4d^9 4s^2 5p\ ^1P_1$ ($\Delta E = 12.810$ eV).

Table 1. DCSs for the $^3P_1$ and $^1P_1$ autoionizing states of Cd at 40 eV incident electron energy (the values in parentheses are statistical errors converted to the absolute scale). At the bottom of the table are integral (Q_I), momentum transfer (Q_M) and viscosity (Q_V) cross sections in 10^{-23} m^2 (the values in parentheses are relative errors).

Scattering angle (degrees)	DCS (10^{-23} m^2 sr^{-1})			
	$4d^9 4s^2 5p\ ^3P_1$	Absolute error	$4d^9 4s^2 5p\ ^1P_1$	Absolute error
2	504(18)	108	2900(200)	646
4	379(12)	81	2180(20)	461
6	289(5)	61	1760(10)	372
8	—	—	1280(70)	279
10	149(4)	32	921(44)	199
20	23.8(2.2)	5	141(11)	32
30	4.9(0.9)	1.4	25.9(0.6)	7.9
40	1.9(0.6)	0.7	10.0(0.2)	2.9
50	0.89(0.12)	0.22	5.4(1.1)	1.6
60	0.60(0.10)	0.16	3.5(0.9)	1.2
70	0.59(0.03)	0.13	3.1(0.8)	1.1
80	0.64(0.13)	0.19	2.3(0.6)	0.7
90	0.59(0.06)	0.14	2.5(0.2)	0.6
100	0.42(0.09)	0.12	2.4(0.5)	0.8
110	0.40(0.03)	0.09	2.0(0.5)	0.7
120	0.39(0.06)	0.10	1.4(0.4)	0.5
130	0.58(0.12)	0.17	1.7(0.6)	0.7
140	0.77(0.05)	0.17	2.5(0.8)	0.9
150	1.09(0.14)	0.27	3.9(1.0)	1.4
Q_I	59(0.27)	16	340(0.27)	92
Q_M	18(0.28)	5.0	96(0.32)	31
Q_V	23(0.28)	6.4	140(0.28)	39

while the momentum transfer $Q_M(n = 1)$ and viscosity $Q_V(n = 2)$ cross sections applying

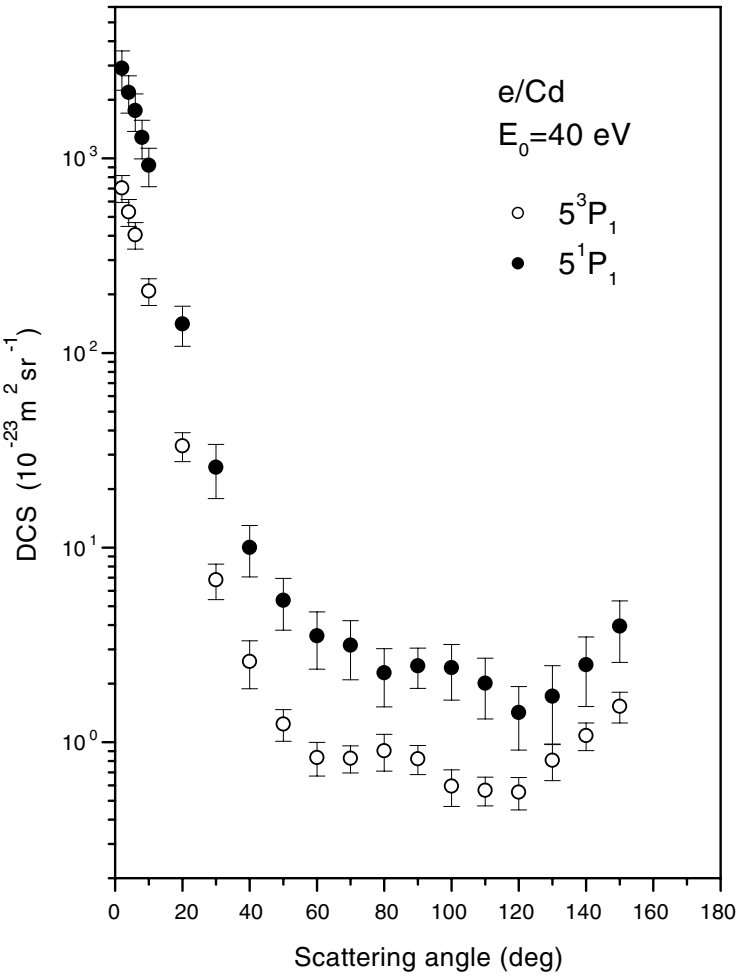

Figure 2. DCSs for electron-impact excitation of the Cd autoionizing states at 40 eV incident electron energy: ○, $4d^9 4s^2 5p\ ^3P_1$; ●, $4d^9 4s^2 5p\ ^1P_1$. Absolute error bars are indicated.

the equation

$$Q_{M(V)} = 2\pi \int_0^{\pi} \mathrm{DCS}(\theta)\left[1 - \left(1 - \frac{\Delta E}{E_0}\right)^{n/2} \cos^n \theta\right] \sin\theta \, \mathrm{d}\theta, \tag{2}$$

where ΔE is the energy loss. Absolute integrated cross section values together with their absolute errors are given at the bottom of table 1. Their relative errors (given in parentheses) arise from the uncertainty of the DCS (0.26) and from extrapolation to 0° and to 180° and numerical integration (0.10).

The absolute DCSs for both the 5 $^3P_1$ and 5 $^1P_1$ states of Cd, with absolute error bars indicated, are shown in figure 2.

3.2. Energy-loss spectra

We have recorded autoionizing energy-loss spectra of Cd at $E_0 = 15$ eV ($\theta = 6°$ and 10°), $E_0 = 18$ eV ($\theta = 10°$), $E_0 = 20$ eV ($\theta = 6°$, 10°, 20° and 40°), $E_0 = 25$ eV ($\theta = 4°$, 6°

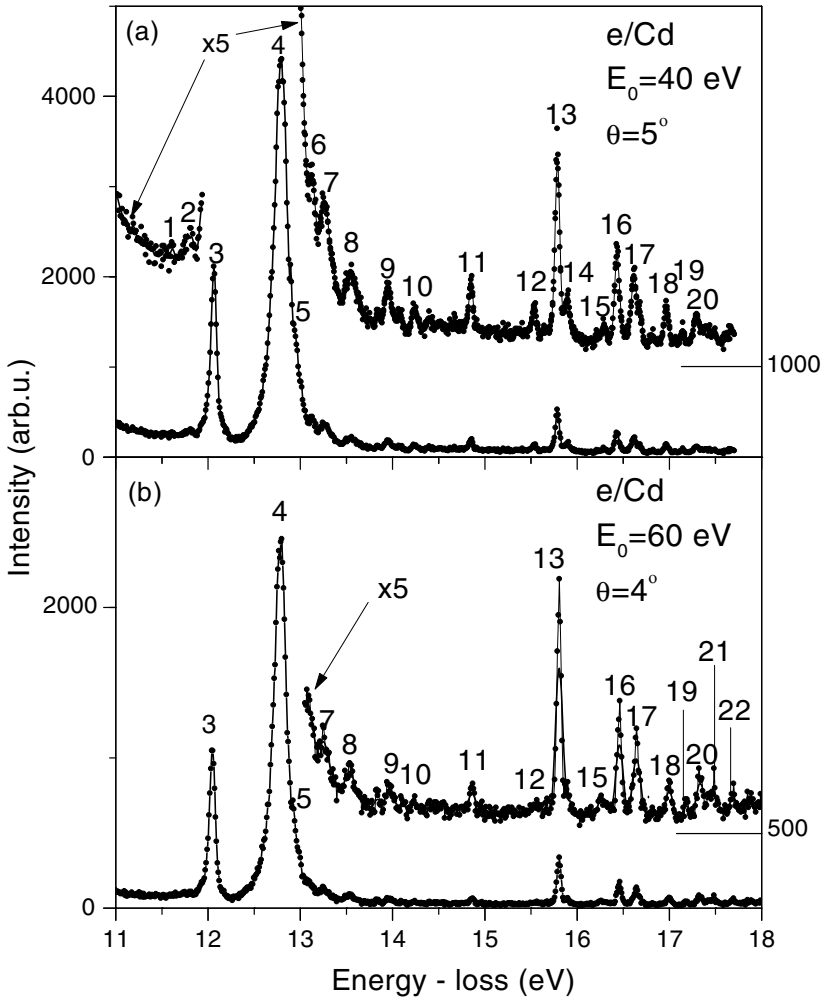

Figure 3. Electron energy-loss spectra of Cd: (a) lower impact energy, $E_0 = 40$ eV ($\theta = 5°$); (b) higher impact energy, $E_0 = 60$ eV ($\theta = 4°$). Above 13 eV, spectra (a) and (b) are also magnified by a factor of five, and shifted by 1000 and 500 units, respectively, for clarity.

and 10°), $E_0 = 40$ eV ($\theta = 5°$, 6° and 20°) and $E_0 = 60$ eV ($\theta = 4°$). The spectra at 40 eV ($\theta = 5°$), and $E_0 = 60$ eV ($\theta = 4°$) are shown in figures 3(a) and (b) respectively. Lines in the spectra are numbered from 1 to 22 in the energy-loss interval of 7 eV, starting from 11 eV. The lines are assigned according to Mansfield and Murnane (1985) and presented in table 2. Our results of the atomic energy levels (as their position in the energy-loss spectra) are presented in the last column of the table. States belonging to the $4d^9 5s^2 5p$ multiplet are positioned at the top of the table and assigned in the form of mixing states, together with dominant states in the *LS* binding scheme. Beside five lines that correspond to this multiplet, other features appear in the spectra. These features attributed to other single- or double-valence excitations of the 'optically allowed' and 'optically forbidden' levels (Mansfield and Murnane 1985) are listed at the bottom in the table.

The isolated feature at 12.062 eV ($5p\ ^3P_1$) in the spectra of Cd at $E_0 = 40$ eV ($\theta = 5°$) and 60 eV ($\theta = 4°$) is fitted using convoluted Gaussian and symmetric Shore functions.

Table 2. Energy levels observed in electron energy-loss spectra of Cd at $E_0 = 40$ eV ($\theta = 5°$) and 60 eV ($\theta = 4°$) in the energy domain from 11 to 18 eV. (Source abbreviations: P1, Pejčev *et al* (1977a); P2, Pejčev *et al* (1977b); MA, Marr and Austin (1969a); M, Mansfield (1978); GC, Garton and Connerade (1969); MM, Mansfield and Murnane (1985).)

	Experiments		Calculation (MM)			This experiment		
Line No	Energy (eV)	Source of data	Energy (eV)	J	Assignment $4d^9 5s^2 5p$ unless otherwise indicated	40 eV $\theta = 5°$	60 eV $\theta = 4°$	Energy (eV)
1	11.634	P1; P2	11.609	2	90% ^{3}P + 7% ^{3}D + 2% $4d^9(5p^3\ ^2P)\ ^3P$	11.605	—	11.605
2	11.804	P1; P2	11.798	3	57% ^{3}F + 35% ^{1}F + 6% ^{3}D + 2% $4d^9(5p^3\ ^2P)\ ^3F$	11.805	—	11.805
3	12.062	MA	12.047	1	81% ^{3}P + 11% ^{1}P + 6% ^{3}D + 2% $4d^9(5p^3\ ^2P)\ ^3P$	12.062	12.062	12.062
	12.064	P1; P2						
4	12.800	MA	12.828	1	85% ^{1}P + 11% ^{3}P + 2% $4d^9(5p^3\ ^2P)^1P$	12.803	12.817	12.810
	12.814	P1; P2						
5	12.939	MA	12.928	1	89% ^{3}D + 6% ^{3}P + 3% $4d^9(5p^3\ ^2P)^3D$	12.936	12.928	12.932
	12.934	P1; P2						
6	13.144	P1; P2	13.141	3	84% 5p5d ^{1}F	13.145	—	13.145
7	13.274	P2	13.221	0	99.7% 5p7s ^{3}P	13.260	13.260	13.260
8	13.544	P2	13.527	1	5p7s(46% ^{1}P + 20% ^{3}P)	13.554	13.542	13.548
	13.527	M						
9	13.954	P2	13.974	1	5p9s(34% ^{3}P + 21% ^{1}P)	13.963	13.945	13.954
	13.944	M						
10	14.234	P2	14.277	1	5p9s(37% ^{1}P + 22% ^{3}P) + 27% 5p5d ^{1}P	14.239	—	14.239
	14.233	M						
11	14.874	P1	14.875	2	6s(57% ^{1}D + 43% ^{3}D)	14.876	14.871	14.874
12	15.574	P1	15.573	2	6s(57% ^{3}D + 43% ^{1}D)	15.560	15.566	15.563
13	15.807	GC	15.799	1	6p(55% ^{1}P + 36% ^{3}P)	15.807	15.807	15.807
	15.809	MA	15.807	2	6p(58% ^{1}D + 30% ^{3}D)			
	15.815	P1	15.816	3	6p(51% ^{3}F + 41% ^{1}F)			
14	15.944	P1	15.939	3	5d(57% ^{1}F + 30% ^{3}F + 11% ^{3}G)	15.930	—	15.930
			15.940	2	5d(56% ^{1}D + 20% ^{3}D + 18% ^{3}F)			
			15.942	4	5d 88% ^{3}F			
15	16.344	P1	16.354	2	7s(59% ^{1}D + 41% ^{3}D)	16.301	16.290	16.295
16	16.454	GC	16.446	0	6p(99.8% ^{3}P)	16.456	16.462	16.459
	16.464	P1	16.448	2	6p(88% ^{3}P + 11% ^{1}D)			
			16.458	1	6p(58% ^{3}P + 40% ^{1}P)			
17	16.641	GC	16.637	1	7p(57% ^{1}P + 31% ^{3}P) or	16.653	16.644	16.649
	16.642	MA						
	16.644	P1	16.631	2	5d(46% ^{3}D + 27% ^{3}P + 23% ^{1}D)			
18	16.993	GC	16.988	1	8p(59% ^{1}P + 31% ^{3}P + 10% ^{3}D)	16.995	16.997	16.996
	16.993	MA						
	17.004	P1						
19	17.177	GC		—	—	17.175	17.167	17.171
	17.178	MA						
	17.184	P1		1	8p ^{1}P (assignment as in P1)			
20	17.318	GC	17.324	1	7p(61% ^{3}P + 38% ^{1}P)	17.328	17.318	17.323
	17.324	P1						
21	17.414	GC	17.413		$4d^9 5s^2(^2D_{3/2})4f[3/2]_1$ (in GC)	—	17.418	17.418
22	17.681	GC	17.686	1	8p(62% ^{3}P + 37% ^{1}P)	—	17.688	17.688
	17.686	MA	17.695	1	89%7p ^{3}D			

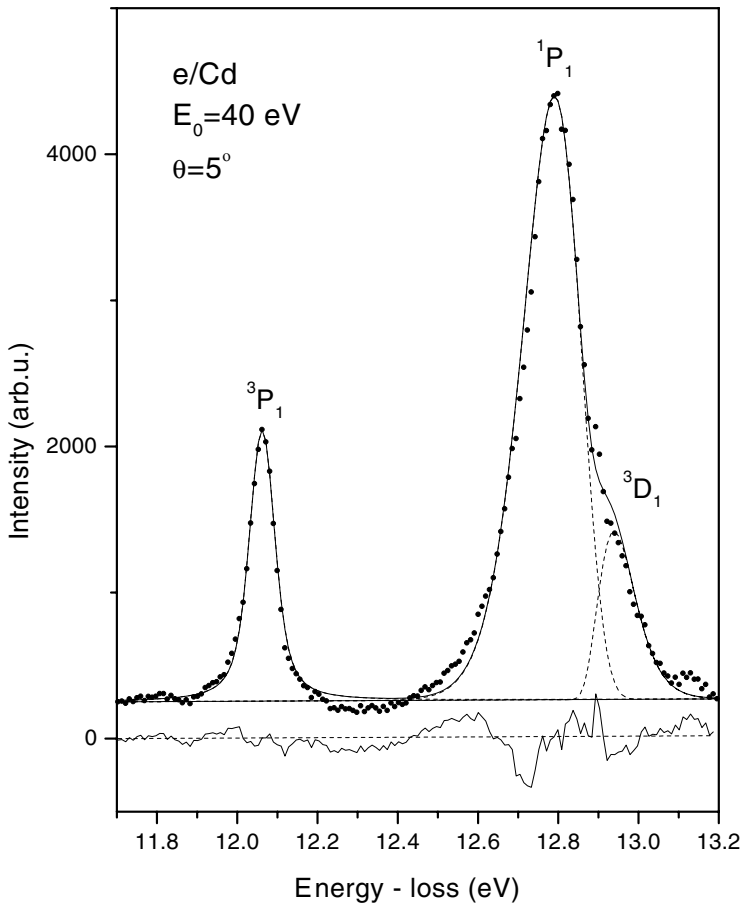

Figure 4. Decomposed energy-loss spectrum of Cd at $E_0 = 40$ eV($\theta = 5°$): ●, raw data; – – –, decomposed states presented using a symmetric Shore function for the $^3P_1$ and log-normal function for both the $^1P_1$ and $^3D_1$, on the baseline; ——, synthetic spectrum. The difference between raw data and the synthetic spectrum is presented at the bottom.

In this case a Gaussian (FWHM of 50 meV) represents our apparatus function. The best fit gives the Shore width of 46.8 and 44.4 meV, respectively, in the two spectra mentioned above. These values are close to the line width obtained by Marr and Austin (1969a) from photoabsorption measurements (44.6 meV) and by Martin *et al* (1996) from their (e, 2e) study (41 meV). The autoionizing 5 $^1P_1$ and 5 $^3D_1$ states are not completely resolved, so we performed decomposition of the feature close to 12.81 eV using two parametric log-normal profiles. In such a way the decomposed spectrum is shown in figure 4. Rather than the parameters, we estimated the FWHM for the 5 $^1P_1$ and 5 $^3D_1$ states as 0.17 eV and <0.1 eV respectively, in relatively good agreement with the 5 $^1P_1$ effective line width (140 meV) obtained by Marr and Austin (1969a). The discrepancy between the effective width of the 5 $^3D_1$ line (<7 meV) determined by Marr and Austin (1969a) and that estimated here (<0.05 eV, after unfolding of the Gaussian FWHM mentioned above and taking into account the contribution of other close states) may indicate difficulties in decomposition.

The spectrum of Zn recorded at $E_0 = 80$ eV ($\theta = 0°$) in a broad energy-loss region (5–14 eV) is shown in figure 5. Above the ionization potential (IP) it contains at least three

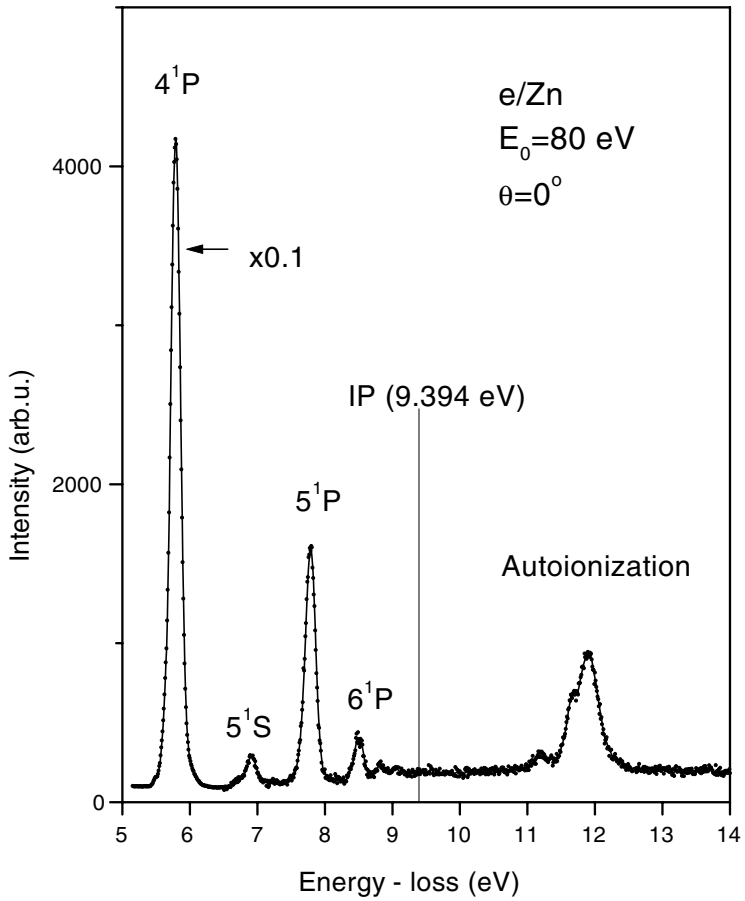

Figure 5. Electron energy-loss spectrum of Zn at $E_0 = 80$ eV ($\theta = 0°$). The 4^1P resonance line is multiplied by 0.1 for clarity. The autoionization region (above the ionization potential, IP) is assigned.

features. The intensity of the $4\ ^1$P resonance peak is more than 40 times larger than that of any separate peak in the autoionizing region. We also recorded energy-loss (from 11.0 to 12.5 eV) autoionizing spectra of Zn at $E_0 = 20$ eV ($\theta = 6°$ and 10°), $E_0 = 60$ eV ($\theta = 4°$, 6° and 10°), $E_0 = 80$ eV ($\theta = 0°$, 4° and 10°) and $E_0 = 100$ eV ($\theta = 0°$).

As an illustration, the autoionizing spectra of Zn at $E_0 = 80$ eV ($\theta = 0°$), $E_0 = 60$ eV($\theta = 4°$) and $E_0 = 20$ eV ($\theta = 10°$) are shown in figure 6, and assigned as (a), (c) and (d), respectively.

4. Discussion and conclusion

We have performed a series of electron spectroscopy measurements of electron collisions with group IIb atoms, at low and medium impact energies (Marinković *et al* 1991, Panajotović *et al* 1993, Panajotović 1999). To our best knowledge, experimental DCSs for Cd autoionizing states at $E_0 = 40$ eV and a broad angular range ($\theta = 2°$–150°) are reported for the first time in this work. The DCSs for both the $5\ ^3P_1$ and the $5\ ^1P_1$ autoionizing states are sharply forward peaked and have two shallow minima: the triplet state at 70° and 120°, the singlet state

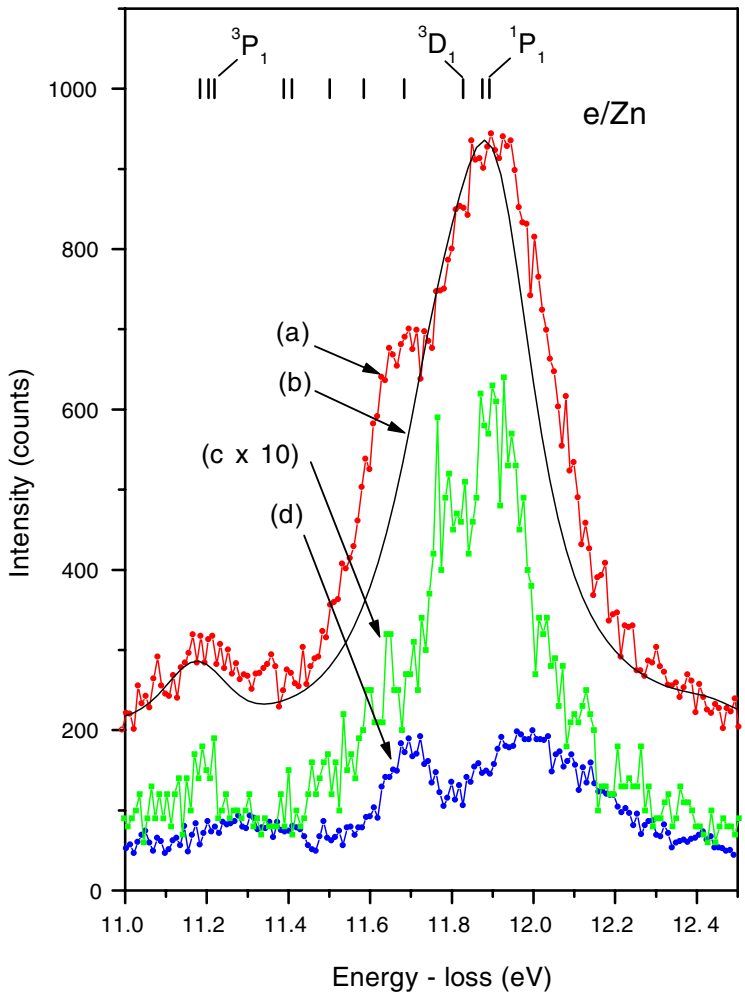

Figure 6. Electron energy-loss spectra of Zn at (a) $E_0 = 80$ eV ($\theta = 0°$), (c) $E_0 = 60$ eV ($\theta = 4°$) multiplied by ten for clarity and (d) $E_0 = 20$ eV ($\theta = 10°$). Full curve (b) represents the photoabsorption spectrum by Marr and Austin (1969b) folded with a Gaussian of FWHM 0.14 eV, the resolution in our experiment. Energies and assignment of the states are according to Mansfield (1981).

at 80° and 120° (5° uncertainty in both cases). Between the minima, these DCSs have local maxima at 100° and 80°, respectively. Unfortunately, agreement between the experimental and theoretical data could not be checked, because there are no available calculated differential or integrated cross sections in this energy region. The angular distributions of ejected electrons for the same lines at $E_0 = 40$ eV, obtained by Pejčev *et al* (1977a), are characteristically different with a maximum at approximately 60° and 70° respectively. Of course, complete analysis is only possible by observing both the scattered and ejected electrons in a coincidence experiment.

Our energy-loss spectra of Cd are in accord with photoabsorption (Marr and Austin 1969a, Mansfield 1978, Garton and Connerade 1969) as well as with ejected-electron (Pejčev *et al* 1977a, 1977b) spectra. The 5 $^3P_1$ autoionizing state in the energy-loss spectra is fitted with a symmetric profile. It assured us that the symmetric component of a Shore line profile is

dominant with respect to the asymmetric. This confirms a high 'line profile index' (Fano 1961) of $q = -20$ obtained by Marr and Austin (1969a). We note a difference in designation of this state by Marr and Austin (1969a) and by Mansfield and Murnane (1985) used in this work.

Decomposition of the 5 $^1P_1$ and the 5 $^3D_1$ autoionizing states using log-normal profiles in this work gave the asymmetry factors: <1 (steeper on the high energy side) and >1 (steeper on the low energy side) respectively. It is in qualitative agreement with the absorption cross section data (Marr and Austin 1969a). This analysis shows (figure 4) that intensity of the 5 $^1P_1$ autoionizing line in the energy-loss spectrum at $E_0 = 40$ eV($\theta = 5°$) is more than six times larger than that of the 5 $^3D_1$ autoionizing line.

Energy-loss spectra of Cd below the IP have been reported earlier (Marinković *et al* 1991). Our DCS for the 5 $^1P_1$ resonance state (at 5.417 eV in our energy-loss spectra) is normalized to the value calculated by Madison *et al* (1991) of 5.6×10^{-18} m^2 sr^{-1} at $E_0 = 40$ eV ($\theta = 5°$). We obtained a DCS for the 5 $^1P_1$ autoionizing state smaller by two orders of magnitude with respect to the 5 $^1P_1$ resonance state (see table 1). It is well known that the total effective cross-section (Q) curve for electron–Zn collision shows lower values than that for electron–Cd collision (Brode 1930), in accord with the general rule that Q is lower if IP is higher. Above the first ionization limits (8.994 eV for Cd and 9.394 eV for Zn) this rule is valid as well. In our laboratory, a DCS of 24×10^{-20} m^2 sr^{-1} for the 4 $^1P_1$ resonance state of Zn at $E_0 = 40$ eV ($\theta = 5°$) was obtained by Panajotović (1999). We estimated that probability for electron-impact excitation of the $(n-1)$d^9ns^2np autoionizing states is remarkably less for Zn ($n = 4$) than for Cd ($n = 5$). It is clear why the overall resolution in this work is lower in recording the energy-loss spectra of Zn than in that of Cd.

We used the energies of the 3d^{9}4s^{2}4p autoionizing states of Zn calculated by Mansfield (1981) to analyse our energy-loss spectra presented in figure 6. A pure dipole photoabsorption spectrum obtained by Marr and Austin (1969b) folded with a Gaussian of FWHM 140 meV (the resolution in our experiment), denoted (b), cannot reproduce our energy-loss spectrum at $E_0 = 80$ eV ($\theta = 0°$), denoted (a) in the same figure. The difference is larger between photoabsorption and our energy-loss spectra at $E_0 = 60$ eV ($\theta = 4°$) and $E_0 = 20$ eV ($\theta = 10°$), denoted in the same figure as (c) and (d) respectively. At lower incident electron energies, the autoionizing states with $J \neq 1$ contribute to the 3d^{9}4s^{2}4p multiplet noticeably, but only tentative assignments of the three states with $J = 1$ are given by Back *et al* (1981). According to Mansfield (1981), several autoionizing states are not identified in the ejected-electron spectra and the state at 11.441 eV is practically the pure 3d^{10}4p^2 ^{1}S ($J = 0$) two-electron excited state. We concluded, from our measurements and analysis, that the states around 11.7 eV with $J \neq 1$ also contribute to our energy-loss spectra, in accord with the low energy ejected-electron spectra.

Trajmar and Williams (1976) reported the Zn energy-loss spectra at $E_0 = 20$ eV ($\theta = 30°$ and 90°) and 40 eV ($\theta = 10°$). Besides ^{3}P, ^{1}P and ^{3}D series of lines belonging to 3d^{9}4s^2mp ($m \geqslant 4$) they observed nine optically forbidden autoionizing states belonging to the 3d^{9}4s^2nl configuration. The feature at 11.60 eV, reported by these authors, obviously appears due to double scattering of incident electrons after successive excitation of the Zn 4 $^1P_1$ resonance state at 5.794 eV. Double scattering was avoided in our experiment by using appropriate temperature of the crucible, as explained in section 2.

The need for more precise experimental knowledge on the Zn autoionizing states could be invoked by the fact that the $^3D_1$ autoionizing state of Zn coincides with the 4s′[1/2]$_1$ state of Ar at 11.828 eV, investigated in detail by Filipović *et al* (2000). A process of selective energy transfer is convenient for 'experimental decomposition' of close-lying lines such as that of the 3d^{9}4s^{2}4p autoionizing states of Zn.

Acknowledgments

We are grateful to Professor Albert Crowe for permanent interest in our work. One of us (DMF) is grateful to the Department of Physics, University of Newcastle, for accommodation during his visit. The Ministry of Science and Technology of the Republic of Serbia, Yugoslavia, have supported this work under project IO1424.

References

Avdonina N B, Felfli Z and Msezane A 1997 *J. Phys. B: At. Mol. Opt. Phys.* **30** 2591
Back C G, White M D, Pejčev V and Ross K J 1981 *J. Phys. B: At. Mol. Phys.* **14** 1497
Berkowitz J and Lifshitz C 1968 *J. Phys. B: At. Mol. Phys.* **1** 438
Beutler H 1933 *Z. Phys.* **87** 19
Beutler H and Guggenheimer K 1933 *Z. Phys.* **87** 176
Brinkman R T and Trajmar S 1981 *J. Phys. E: Sci. Instrum.* **14** 245
Brode R B 1930 *Phys. Rev.* **35** 504
Chutjian A 1979 *Rev. Sci. Instrum.* **50** 347
Doschek G A 1985 *Autoionization* ed A Temkin (New York: Plenum) p 171
Fano U 1961 *Phys. Rev.* **124** 1866
Filipović D M, Marinković B P, Pejčev V and Vušković L 2000 *J. Phys. B: At. Mol. Opt. Phys.* **33** 677
Filipović D, Pejčev V, Marinković B and Vušković L 1988 *Fizika* **20** 421
Garton W R and Connerade J P 1969 *Astrophys. J.* **155** 667
Ivanov I G, Latush E L and Sem M F 1990 *Metal Vapour Ion Lasers* (Moscow: Energoatomizdat) and references therein (in Russian)
Kontros J E, Szoter L, Cherhyshova I V and Shpenik O B 2002 *J. Phys. B: At. Mol. Opt. Phys.* **35** 2195
Madison D H, Bartschat K and Srivastava R 1991 *J. Phys. B: At. Mol. Opt. Phys.* **24** 1839
Mansfield M W D 1978 *Proc. R. Soc.* A **362** 129
Mansfield M W D 1981 *J. Phys. B: At. Mol. Phys.* **14** 2781
Mansfield M W D and Connerade J P 1978 *Proc. R. Soc.* A **359** 389
Mansfield M W D and Murnane M M 1985 *J. Phys. B: At. Mol. Phys.* **18** 4223
Marinković B, Pejčev V, Filipović D and Vušković L 1991 *J. Phys. B: At. Mol. Opt. Phys.* **24** 1817
Marr G V and Austin J M 1969a *Proc. R. Soc.* A **310** 137
Marr G V and Austin J M 1969b *J. Phys. B: At. Mol. Phys.* **2** 107
Martin N L S 1984 *J. Phys. B: At. Mol. Phys.* **17** 1797
Martin N L S, Bauman R P, Thomson D B, Wilson M and Ross K J 1996 *J. Phys. B: At. Mol. Opt. Phys.* **29** 4457
Martin N L S, Bauman R P and Wilson M 1999 *Phys. Rev.* **59** 2764
Martin W C, Sugar J and Tech J L 1972 *J. Opt. Soc. Am.* **62** 1488
Mies F H 1968 *Phys. Rev.* **175** 164
Newell W R, Ross K J and Wickes J B 1973 *J. Phys. B: At. Mol. Phys.* **6** L337
Panajotović R 1999 *PhD Thesis* Faculty of Physics, University of Belgrade
Panajotović R, Pejčev V, Konstantinović M, Filipović D, Bočvarski V and Marinković B 1993 *J. Phys. B: At. Mol. Opt. Phys.* **26** 1005
Pejčev V, Rassi T W and Ross K J 1977b *J. Phys. B: At. Mol. Phys.* **10** L629
Pejčev V, Ross K J, Rassi T W and Ottley T W 1977a *J. Phys. B: At. Mol. Phys.* **10** 459
Ross K and Sonntag B 1998 *Rev. Sci. Instrum.* **66** 4409
Shore B V 1967 *Rev. Mod. Phys.* **39** 449
Tabanli M M, Peacher J L and Madison D H 2002 *Phys. Rev.* A **65** 042718
Trajmar S and Williams W 1976 VIII SPIG *Physics of Ionized Gases* ed B Navinšek (Ljubljana: University of Ljubljana Press) p 199
Wickes J B P, Ross K J and Newell W R 1971 *J. Phys. B: At. Mol. Phys.* **4** L26
Wilson M 1968 *J. Phys. B: At. Mol. Phys.* **1** 736